

Modeling Drug Release from Materials Based on Electrospun Nanofibers

Paweł Nakielski^{1*}, Tomasz Kowalczyk¹, Tomasz A. Kowalewski¹

¹Institute of Fundamental Technological Research Polish Academy of Sciences

*Corresponding author: 5B Pawinskiego Str., 02-106 Warsaw, Poland, pnakiel@ippt.pan.pl

Abstract: Comprehensive studies of drug transport in nanofibres based mats have been performed to predict drug release kinetics. The paper presents our approach to analyze the impact of fibers arrangement, one of the parameters varied in our parallel experimental studies. Drug encapsulation in submicron fibers and subsequent controlled release of drugs is a tedious task due to the large number of process and material parameters involved. In the numerical study we constructed a 3D finite element geometry representing nanofibrous cubic element. COMSOL Multiphysics has been used to assess the impact of the various purposed arrangements of fibers within the mat. Drug release from nanofibers was modeled by adsorption - desorption and diffusion equation, where drug diffusion coefficient in the fluid between the fibers was altered depending on porosity of the material. Our study shows that for the same material porosity drug release from the matrix of regularly oriented fibers is slower than from randomly oriented, isotropic nanofibrous material. Also by decreasing distance between the fibers drug transport rate is reduced.

Keywords: desorption, drug delivery, nanofibers

1. Introduction

Electrospun nanofibers are prospective medicament carriers suitable for local administration of drugs in a controlled manner. Non-woven nanofibrous mats have shown potential for the use in transdermal delivery systems¹ and as implants releasing bioactive molecules including proteins^{2,3}, anticancer drugs⁴ or antioxidants^{1,5}. Besides physical transport phenomena, chemical reactions may affect drug release kinetics. Here, we only consider systems in which the drug is physically immobilized within water-insoluble polymeric matrix of specifically structured nanofibers. The expected drug release time is of order of weeks. However, at this step we neglect long term effects due to the polymer degradation. Nanofibers are obtained by electrospinning of polymer solutions. Here, the process parameters, like applied voltage, pumping rate, collector characteristics, solution composition strongly affects formation of fibers, and can be varied to modify fibers diameter, porosity of fibers and

collected mats, as well as fibers orientation. A very important aspect of controlling the drug release kinetics is method of drug encapsulation. In the simplest case of a lipophilic drug and polymer, fibers formed during electrospinning of a solution have uniformly distributed drug in the cross-section. On the other hand encapsulation of the hydrophilic proteins can be only performed using core-shell or micro-emulsion methods. Here, protein solution is coaxially electrospun or entrapped as small droplets within the polymer solution, which after solidification forms membrane like mats, consequently applied as drug carriers in medical applications⁶.

Applied mathematical model with adsorption-desorption kinetic on the surface of the fibers together with non-sink conditions on two external planes of cubic geometry can account for not complete release of the drug from the matrix, what can be seen in the experimental results.

This work contains our attempts to estimate impact of structural parameters on drug release from the materials currently applied as protective mats for neurosurgery. Such model construction can be applied for fitting the kinetics of drug release and to help find optimal geometry and structure of the nanofibrous mats avoiding tedious experimental tests.

2. Mathematical formulation

For the analysis of drug release, simulations were carried out in a cubic element representing small section of a nanofibrous mat. Dimension of the element results from observations of typical thickness of electrospun materials and was set to $L = 100\mu\text{m}$. In the cubic element 15×15 cylindrical fibers were placed. In the first geometry regular configuration of parallel fibers of average diameter $r = 2.0\mu\text{m}$ is studied (Fig.1). Porosity of the created material geometry is equal $\varepsilon = 0.72$. It is close to the experimental value obtained by comparing average specific density of the material and that of the polymer:

$$\varepsilon = 1 - \frac{\rho_m}{\rho_p} \quad (1)$$

where ρ_m is average material density (kg/m^3), ρ_p is polymer density (kg/m^3).

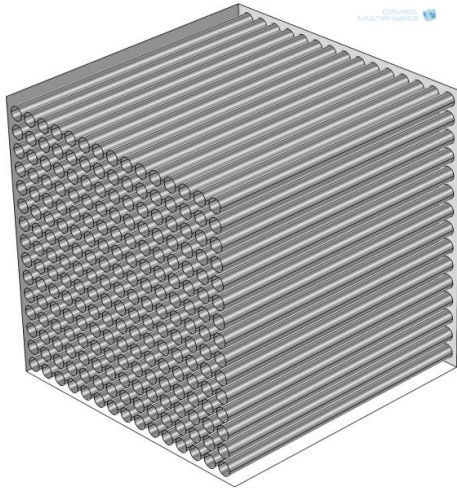


Figure 1. Geometry of regularly spaced fibers, $r = 2.0\mu\text{m}$, $\varepsilon = 0.72$, $\mathbf{K}_t = [1 \ 0 \ 0]$.

In case of material with irregular fibers placement, the two geometries were created. For this purpose, cylinder position and direction coordinates were randomly selected to achieve two different distributions of fibers orientation: moderately disturbed parallel fibers orientation (Fig. 2) and completely random fibers orientation (Fig. 3). The fibers orientation was described using second order tensor \mathbf{K}_t proposed by Stylianopoulos⁷. In the ideal case of fully randomly oriented fibers, trace of the tensor equals $\mathbf{K}_t = [1/3, 1/3, 1/3]$ (note that the sum of tensor components must be equal to unity). If one of the directions becomes dominant, trace of the tensor appropriately varies.

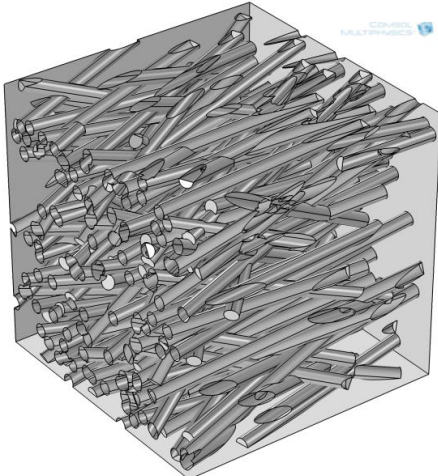


Figure 2. Geometry of moderately oriented fibers, $r = 2.0\mu\text{m}$, $\varepsilon = 0.72$, $\mathbf{K}_t = [0.70 \ 0.14 \ 0.16]$.

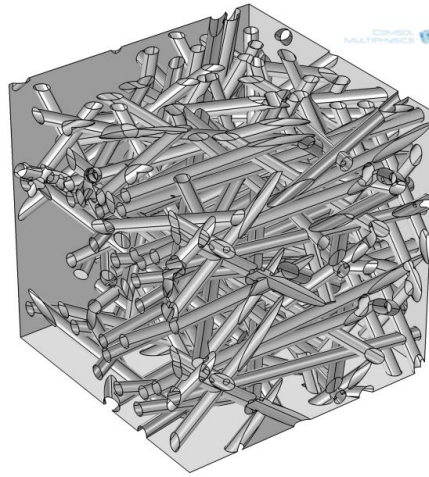


Figure 3. Geometry of randomly oriented fibers, $r = 2.0\mu\text{m}$, $\varepsilon = 0.72$, $\mathbf{K}_t = [0.36 \ 0.33 \ 0.31]$.

The transient sorption process applied in the numerical model is a Langmuir bimolecular process between drug molecule C_A and unoccupied site $(C_B^{\text{max}} - C_B)$, where C_B^{max} is maximal concentration of adsorbed drug.

Necessary assumptions have been applied in the model:

- drug can form single layer on the fiber surface,
- every empty adsorption site is equivalent,
- no degradation of polymeric fiber occurs during release period,
- at the beginning of the release process drug is distributed homogeneously,
- diffusion of the drug in the fluid is described by Fick's law.

The change of drug concentration on the fiber surface can be represented by adsorption and desorption terms with constant rates k_{ads} , k_{des} , respectively:

$$\frac{\partial C_B}{\partial t} = k_{\text{ads}} \cdot C_A \cdot (C_B^{\text{max}} - C_B) - k_{\text{des}} \cdot C_B \quad (2)$$

where C_B is drug concentration expressed in relation to the weight of the polymer material (kg/kg), C_A is drug concentration in the fluid (kg/m³).

Spatiotemporal distribution of the drug in the fluid surrounding fibers is described by diffusion equation and additional mass source term describing drug released from the fibers:

$$\frac{\partial C_A}{\partial t} = D_A \nabla^2 C_A + \rho_p \cdot \frac{\partial C_B}{\partial t} \quad (3)$$

where ρ_p is polymer density (kg/m³).

Flux boundary condition was applied on two opposite sides of the nanofibrous mat which contacts considered element with external fluid:

$$N_S = k_c(c_A - c_A^{out}) \quad (4)$$

where c_A^{out} is drug concentration outside considered element and in our case is equal zero, k_c is the mass transfer coefficient. On the remaining walls of cubic element, Neumann boundary conditions were applied which corresponds to symmetry condition in the normal direction to the surface \vec{n} :

$$D_A \nabla c_A \cdot \vec{n} = 0 \quad (5)$$

Initial concentration of the drug on the fibers surface is $c_B = c_B^{max} = c_{B0}$ and $c_{A0} = 0$ for the fluid. After the immersion of the material, release process starts and continues until equilibrium state is reached.

Diffusion coefficient for the drug in fluid is constant. This coefficient is calculated from semi empirical equation (6) which takes into account porosity of fibrous material, drug molecule and fiber diameter ratio. For the calculation of diffusion coefficient we used semi empirical equation proposed Clague and Phillips⁸, which takes into account hydrodynamic and steric effects:

$$\frac{D_A}{D_0} = F \cdot S = e^{-a \cdot (1-\varepsilon)^b} \cdot e^{-0.84 \cdot f^{1.09}} \quad (6)$$

where D_A/D_0 express the ratio of diffusion coefficients in fluid with and without presence of the fibers, ε - porosity of the material, $f = (1-\varepsilon) \cdot (1+\lambda)^2$ - corrected volume fraction expressed by λ - ratio of drug molecule calculated from Einstein - Smoluchowski equation and fiber diameter r ($r_m = 0.9$ nm, $r = 2.0\mu\text{m}$; $\lambda = 0.00045$). Coefficient a and b were specified by Amsden et al. and equals $a = \pi$, $b = 0.174 \cdot \ln\left(\frac{59.6}{\lambda}\right) = 2.05$. Figure 4 presents diffusion coefficients ratio dependence on different drug molecule and fiber ratio.

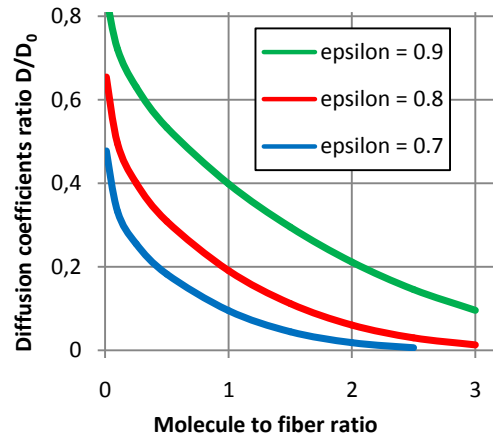


Figure 4. Variation of the relative diffusion coefficients for three different porosities of the material in the function of drug molecule to fiber ratio.

3. Use of COMSOL Multiphysics

The model of nanofibrous mat was designed and simulated using COMSOL Multiphysics. Moderately aligned and randomly oriented fibers have been generated using separate program to create geometry of 225 fibers predefined average orientation and its standard deviation. These fibers were subtracted from the cubic computational domain. Finally, approximately 650 000 tetrahedral mesh elements were formed. The application modes used for drug delivery simulations was Transport of Diluted Species modules with two dependent variables. Considered drug release time was 14 days and Direct MUMPS solver was used to solve presented system of equations.

4. Results and Discussion

Simulations of drug release were performed with kinetic parameters and initial concentration values found for typical experiments performed in our laboratory to mimic such process. For this purpose Rhodamine B released from poly(L-lactide-co-ε-caprolactone) nanofiber mats was studied using especially designed optical setup. Diffusion coefficient of Rhodamine B in water was measured in $T = 37^\circ\text{C}$ using Fluorescence After Photobleaching method and its value is consistent with the data found in the literature^{9,10}.

Three kinetic parameters were fitted with experimental data and their values are presented in Table 1.

Table 1: Values of parameters used in study

Parameter	Value
Diffusion coefficient - D_A	$2.2 \cdot 10^{-10} \text{ m}^2/\text{s}$
Diffusion coefficient - D_0	$5.1 \cdot 10^{-10} \pm 0.9 \text{ m}^2/\text{s}$
Adsorption constant - k_{ads}	$1 \cdot 10^{-6} \text{ m}^3/(\text{kg} \cdot \text{s})$
Desorption constant - k_{des}	$1 \cdot 10^{-5} \text{ 1/s}$
Mass transfer coefficient - k_c	$1 \cdot 10^{-9} \text{ m/s}$
Drug concentration on the fiber surface - C_{B0}	$1 \cdot 10^{-2} \text{ kg/kg}$

Figure 5 presents cumulative release profile for four types of fiber arrangement. The slowest release was achieved for material with regular, locally concentrated fibers. In this case fibers were moved close to each other to demonstrate their coordinated effect on drug release. In this case distance between fibers was set to $0.2 \mu\text{m}$. As presented in Figure 6 for this configuration locally high values of concentration can occur.

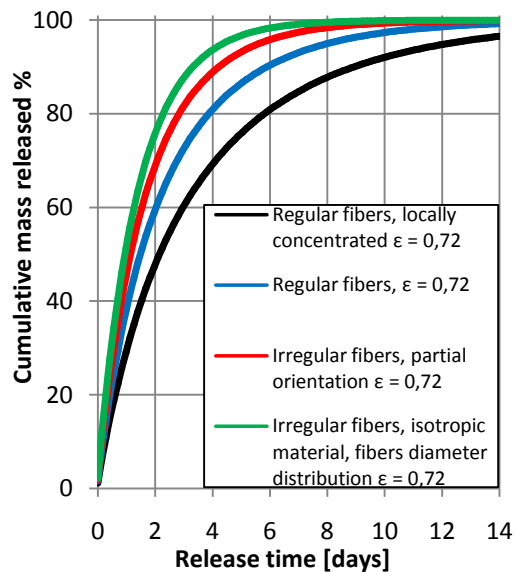


Figure 5. Simulated drug release profile. Dependence on different fiber arrangement

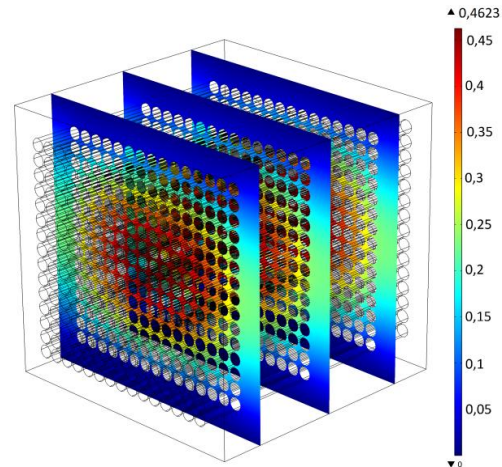


Figure 6. Simulated drug concentration distribution in fluid between regular, concentrated fibers after 14 days of release $r = 2.0 \mu\text{m}$, $\mathbf{K}_t = [1 \ 0 \ 0]$.

Regularly arranged, uniformly spaced fibers released the same mass of drug in longer time. Increase in spacing between fibers (Fig.7) allowed diffusion to transport compound to boundary connected with external fluid. Much faster release can be observed for irregular fiber composition. Material with moderately oriented fibers (Fig.8) has bigger pores and transport resistance is much smaller. The fastest release was found for irregular fibers arrangement (Fig.9) with no dominant fiber orientation. In this case drug transport towards the boundary connected with the liquid was the least affected by the fibers.

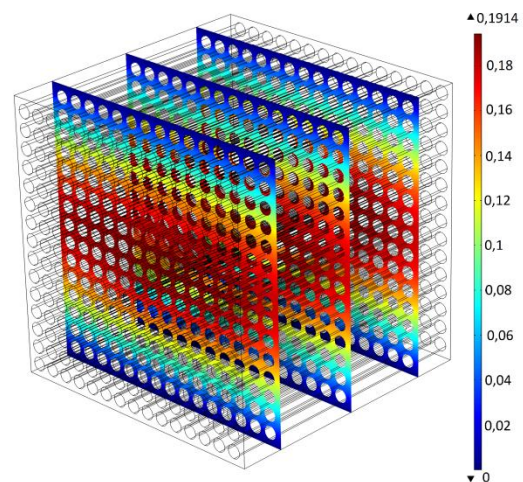


Figure 7. Simulated drug concentration distribution in fluid between regular fibers after 14 days of release $r = 2.0 \mu\text{m}$, $\mathbf{K}_t = [1 \ 0 \ 0]$.

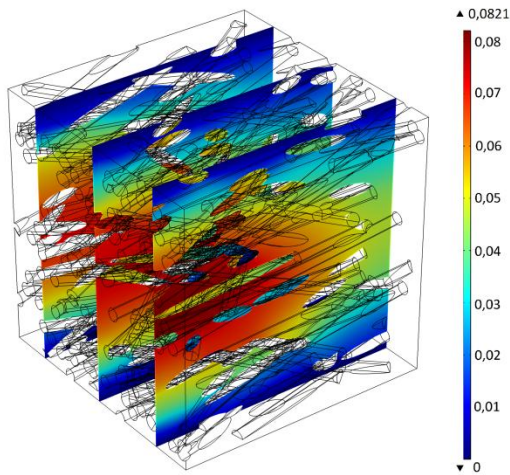


Figure 8. Simulated drug concentration distribution in fluid between moderately oriented fibers after 14 days of release $r = 2.0\mu\text{m}$, $\mathbf{K}_t = [0.70 \ 0.14 \ 0.16]$.

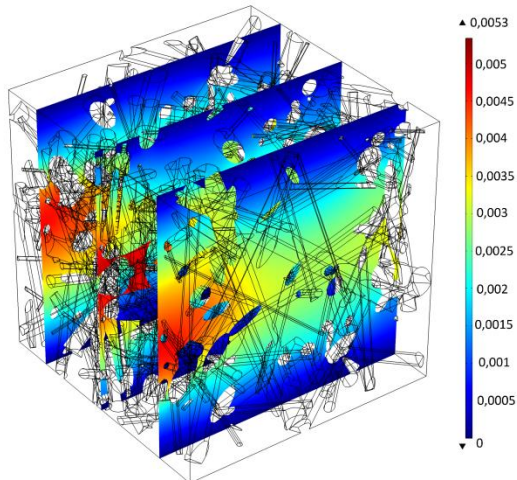


Figure 9. Simulated drug concentration distribution in fluid between randomly oriented fibers after 14 days of release $r = 2.0\mu\text{m}$, $\mathbf{K}_t = [0.36 \ 0.33 \ 0.31]$.

To provide overall characteristic of presented model, parametric study was performed for three important parameters: diffusion constant, mass transfer coefficient and desorption rate. In every case variable values were changed of the order of magnitude.

A higher value of the diffusion coefficient did not increase the rate of drug release and is not shown. Reduction of the diffusion coefficient (Fig.10) by one order of magnitude did not affect significantly the transport process, however smaller values of diffusion coefficient decreased drug release extensively. This implies that if one intends to prolong drug release, the use of larger

drug molecules can help to achieve desired effect. Another option may be an attempt to reduce the porosity of the material what can significantly affect the diffusion process.

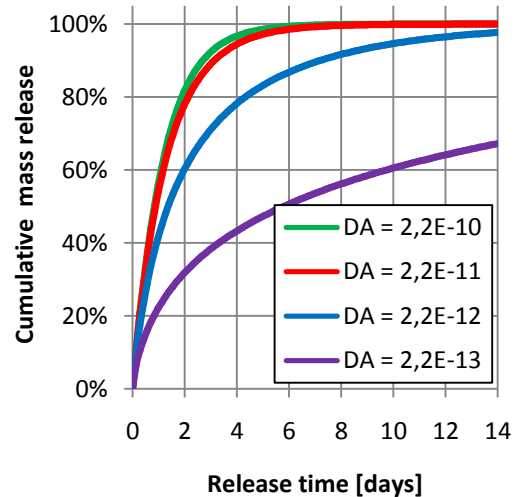


Figure 10. Simulated drug release profile. Dependence on different diffusion coefficients.

Change of mass transfer coefficient (Fig.11) may inhibit release from the material at certain moment. Presented course of the release curve is often observed in the analysis of materials produced in our laboratory and may arise due to the interaction between the polymer and the drug.

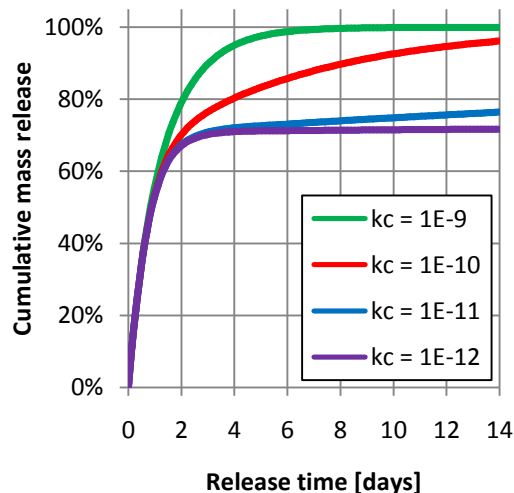


Figure 11. Simulated drug release profile. Dependence on different mass transfer coefficient.

Increase of desorption rate constant (Fig.12) enhanced drug transport and caused undesirable effect of burst release, where approx. 80% of drug was released in first few hours. Decrease of these constant makes that the process is controlled only by desorption.

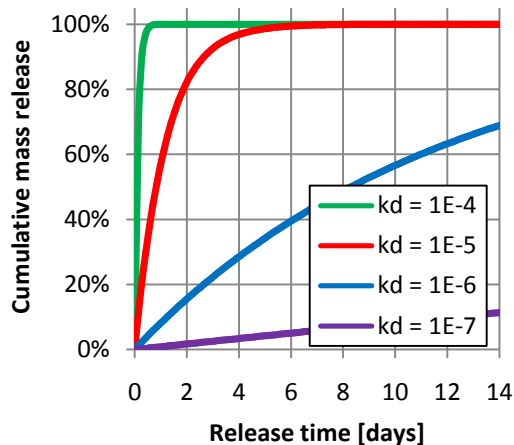


Figure 12. Simulated drug release profile. Dependence on different drug desorption rate.

5. Conclusions

Results of presented simulations show that for the same material porosity drug release from the matrix of regularly oriented fibers is slower than from randomly oriented, isotropic nanofibrous material. Also by decreasing distance between the fibers drug transport rate is reduced. It means that if one intends to inhibit drug release in a given direction, highly oriented fibers constituting the outer barrier of a mat can help to reduce selectively its diffusive transport. Also the use of drugs having high molar masses can slow release process. The model predicts the occurrence of the observed effects in the analysis of materials. Especially the so-called burst release of the drug, and can also describe a case where the cumulative dose released is less than 100%.

6. References

1. Taepaiboon, P., Rungsardthong, U. & Supaphol, P. Vitamin-loaded electrospun cellulose acetate nanofiber mats as transdermal and dermal therapeutic agents of vitamin A acid and vitamin E. *European journal of pharmaceuticals and biopharmaceutics*. V **67**, 387–97 (2007).

2. Srouji, S. *et al.* Slow-Release Human Recombinant Bone Morphogenic Protein-2 Embedded Within Electrospun Scaffolds for Regeneration of Bone Defect: In Vitro and In Vivo Evaluation. *Tissue Engineering: Part A* **17**, 269–277 (2011).
3. Chew, S. Y., Wen, J., Yim, E. K. F. & Leong, K. W. Sustained release of proteins from electrospun biodegradable fibers. *Biomacromolecules* **6**, 2017–24 (2005).
4. Zheng, F., Wang, S., Shen, M., Zhu, M. & Shi, X. Antitumor efficacy of doxorubicin-loaded electrospun nano-hydroxyapatite-poly(lactic-co-glycolic acid) composite nanofibers. *Polymer Chemistry* **4**, 933 (2013).
5. Wu, X.-M., Branford-White, C. J., Yu, D.-G., Chatterton, N. P. & Zhu, L.-M. Preparation of core-shell PAN nanofibers encapsulated α -tocopherol acetate and ascorbic acid 2-phosphate for photoprotection. *Colloids and surfaces. B, Biointerfaces* **82**, 247–52 (2011).
6. Andrychowski, J. *et al.* Nanofiber nets in prevention of cicatrization in spinal procedures. Experimental study. *Folia Neuropathologica* **2**, 147–157 (2013).
7. Stylianopoulos, T., Diop-Frimpong, B., Munn, L. L. & Jain, R. K. Diffusion anisotropy in collagen gels and tumors: the effect of fiber network orientation. *Biophysical journal* **99**, 3119–28 (2010).
8. Clague, D. S. & Phillips, R. J. Hindered diffusion of spherical macromolecules through dilute fibrous media. *Physics of Fluids* **8**, 1720 (1996).
9. Gendron, P.-O., Avaltroni, F. & Wilkinson, K. J. Diffusion coefficients of several rhodamine derivatives as determined by pulsed field gradient-nuclear magnetic resonance and fluorescence correlation spectroscopy. *Journal of fluorescence* **18**, 1093–101 (2008).
10. Shkilnyy, A., Proulx, P., Sharp, J., Lepage, M. & Vermette, P. Diffusion of rhodamine B and bovine serum albumin in fibrin gels seeded with primary endothelial cells. *Colloids and surfaces. B, Biointerfaces* **93**, 202–7 (2012).

7. Acknowledgements

This study was supported by the National Centre for Research and Development Project #NR13008110. The first author has been supported with a scholarship from the European Social Fund, Human Capital Operational Programme.